Published in final edited form as:

Cancer Discov. 2016 August ; 6(8): 886–899. doi:10.1158/2159-8290.CD-15-0947.

GM-CSF Mediates Mesenchymal–Epithelial Cross-talk in Pancreatic Cancer

Meghna Waghray[1,2,3], **Malica Yalamanchili**[1,3], **Michele Dziubinski**[1,3], **Mina Zeinali**[3,4], **Marguerite Erkkinen**[1,3], **Huibin Yang**[1,2,3], **Kara A. Schradle**[1,2], **Sumithra Urs**[1,2,3], **Marina Pasca Di Magliano**[1,2], **Theodore H. Welling**[1,3], **Phillip L. Palmbos**[3,5], **Ethan V. Abel**[1,2,3], **Vaibhav Sahai**[1,2,3,5], **Sunitha Nagrath**[2,3,4], **Lidong Wang**[1,2,3], and **Diane M. Simeone**[1,2,3,6]

[1]Department of Surgery, University of Michigan, Ann Arbor, Michigan

[2]Pancreatic Cancer Center, University of Michigan, Ann Arbor, Michigan

[3]Translational Oncology Program, University of Michigan, Ann Arbor, Michigan

[4]Department of Chemical Engineering, University of Michigan, Ann Arbor, Michigan

[5]Department of Internal Medicine, University of Michigan, Ann Arbor, Michigan

[6]Department of Molecular and Integrative Physiology, University of Michigan, Ann Arbor, Michigan

Abstract

Pancreatic ductal adenocarcinoma (PDA) is characterized by a dense stroma consisting of a prevalence of activated fibroblasts whose functional contributions to pancreatic tumorigenesis remain incompletely understood. In this study, we provide the first identification and characterization of mesenchymal stem cells (MSC) within the human PDA microenvironment, highlighting the heterogeneity of the fibroblast population. Primary patient PDA samples and low-passage human pancreatic cancer–associated fibroblast cultures were found to contain a unique population of cancer-associated MSCs (CA-MSC). CA-MSCs markedly enhanced the growth, invasion, and metastatic potential of PDA cancer cells. CA-MSCs secreted the cytokine GM-CSF

Corresponding Author: Diane M. Simeone, University of Michigan, 1500 East Medical Center Drive, 2910B Taubman Center, SPC 5343, Ann Arbor, MI 48109-5343. Phone: 734-615-1600; Fax: 734-647-6977; simeone@med.umich.edu.

Note: Supplementary data for this article are available at Cancer Discovery Online (http://cancerdiscovery.aacrjournals.org/).

Disclosure of Potential Conflict of Interest
No potential conflicts of interest were disclosed.

Authors' Contributions
Conception and design: M. Waghray, D.M. Simeone
Development of methodology: M. Waghray, M. Yalamanchili, T.H. Welling, E.V. Abel, S. Nagrath, D.M. Simeone
Acquisition of data (provided animals, acquired and managed patients, provided facilities, etc.): M. Waghray, M. Yalamanchili, M. Dziubinski, M. Zeinali, H. Yang, K.A. Schradle, S. Urs, L. Wang, D.M. Simeone
Analysis and interpretation of data (e.g., statistical analysis, biostatistics, computational analysis): M. Waghray, M. Pasca Di Magliano, T.H. Welling, P.L. Palmbos, E.V. Abel, S. Nagrath, L. Wang, D.M. Simeone
Writing, review, and/or revision of the manuscript: M. Waghray, M. Pasca Di Magliano, T.H. Welling, P.L. Palmbos, E.V. Abel, V. Sahai, D.M. Simeone
Administrative, technical, or material support (i.e., reporting or organizing data, constructing databases): M. Yalamanchili, M. Zeinali
Study supervision: S. Nagrath, D.M. Simeone
Other (provided cell lines and helped with animal work): M. Dziubinski
Other (helped with in vitro experiments): M. Erkkinen

that was required for tumor cell proliferation, invasion, and transendothelial migration. Depletion of GM-CSF in CA-MSCs inhibited the ability of these cells to promote tumor cell growth and metastasis. Together, these data identify a population of MSCs within the tumor microenvironment that possesses a unique ability, through GM-CSF signaling, to promote PDA survival and metastasis.

SIGNIFICANCE—The role of stroma in pancreatic cancer is controversial. Here, we provide the first characterization of MSCs within the human PDA microenvironment and demonstrate that CA-MSCs promote tumorigenesis through the production of GM-CSF. These data identify a novel cytokine pathway that mediates mesenchymal–epithelial cross-talk and is amenable to therapeutic intervention.

INTRODUCTION

Pancreatic ductal adenocarcinoma (PDA) is an almost uniformly fatal malignancy characterized by the pathognomonic histologic feature of a profound desmoplastic stroma. The PDA stroma, which often constitutes over 80% of the tumor volume, is heterogeneous and comprised of both cellular and acellular components. The cellular component mostly consists of mesenchymal-appearing spindle-shaped cells [often termed cancer-associated fibroblasts (CAF)], immune cells, and vascular cells. Acellular components within the PDA stroma include extracellular matrix and soluble proteins such as cytokines and growth factors (1). It has been hypothesized that the stroma contributes to the aggressive nature of PDA; however, the precise role of the stroma in pancreatic tumorigenesis remains controversial. The predominant stromal cell type is CAFs, but whether all CAFs are similar and how they contribute to tumorigenesis is incompletely understood. Earlier studies using *in vitro* assays, xenografts, and genetically engineered mouse models have suggested that activated stromal cells promote tumor growth and metastasis (2–6). In some studies, patients with pancreatic cancer with high stromal activity, measured by increased α-smooth muscle actin (α-SMA)–expressing myofibroblast cells within their tumors, have worse overall survival (7, 8). In contrast, others have proposed that the stroma may possess a protective role in “restraining” tumor cells. Stromal reduction as a result of Sonic Hedgehog (Shh) deletion in the pancreatic epithelium or via genetic depletion of proliferating α-SMA–expressing myofibroblasts using a thymidine kinase–mediated strategy led to more aggressive and undifferentiated tumors with enhanced metastatic capacity in genetically engineered mice (9, 10). In accordance with these reports, a retrospective study in patients with PDA demonstrated a strong correlation between high collagen deposition and enhanced patient survival (7). The controversy in these studies may be, at least in part, due to a limited understanding of the components of the stroma and their contribution to the biological behavior of pancreatic cancer.

Recently, studies in several solid cancer types have reported that mesenchymal stem cells (MSC) are present in the tumor stroma (11–13). In ovarian cancer, MSCs isolated from the tumor stroma were found to regulate cancer stem cells (CSC) and tumorigenesis via increased BMP production (12). More recently, colon cancer MSCs were determined to modulate the tumorigenicity of colon cancer cells through IL6 (13). In the present study, we

isolate MSCs from primary human pancreatic cancers and pursue a mechanistic study to understand their unique contribution to pancreatic tumorigenesis.

RESULTS

Isolation of Primary Human Pancreatic Cancer–Associated MSCs

To understand the heterogeneity of the mesenchymal cells in the tumor microenvironment of human PDA, we isolated human pancreatic CAFs from primary PDA tumors ($n = 15$) using a culture outgrowth method. We confirmed that the isolated CAFs were not contaminated with neoplastic epithelial cells (CK19) and immune cells (CD45) by IHC analysis, whereas CK19- and CD45-expressing cells were present in matching sections of the primary tumors (Fig. 1A). CAF cultures did not contain the endothelial and immune markers CD34 and CD14 (data not shown). Cancer cells that have undergone epithelial–mesenchymal transition (EMT) might also be a source of mesenchymal-appearing cells from the PDA stroma (14). To rule out this possibility, we assessed KRAS mutational status and identified KRAS mutations in the cancer cells but not in matching CAF cells, demonstrating that CAF cultures did not contain neoplastic epithelial cells that had undergone EMT (Fig. 1B). We found that all CAF cells expressed the stromal markers α-SMA, vimentin, and fibroblast-associated protein (FAP; Fig. 1C); however, there was heterogeneity in the degree of expression of each marker among cells within the CAF cultures (Fig. 1C). Similar to cultured CAFs, we found mesenchymal cells coexpressing α-SMA and FAP, and vimentin and FAP, in matching sections of primary tumors (Fig. 1C).

Based on the heterogeneity of marker expression in the CAF cultures, we hypothesized that distinct cell populations might exist within this stromal compartment. MSCs have been recently described to be a part of the tumor microenvironment in several tumor types (11–13), and MSCs have been described in the pancreas of normal mice and humans (15, 16), but their presence in the neoplastic pancreas has not previously been investigated. We therefore assessed if an MSC population was present in the primary PDA-derived CAF cultures. Flow cytometric analysis was performed to examine the expression of a series of markers routinely used to identify MSCs, including CD90, CD49α, CD44, and CD73 (17). In each of the 15 low-passage PDA-derived CAF cultures, we identified an MSC population expressing all four markers [cancer-associated MSC (CA-MSC); Supplementary Table S1]. An example of a CAF line is shown in Fig. 1D, where 6.9% of total CAFs expressed all 4 MSC markers. Of note, heterogeneity in the percentage of CA-MSCs within individual tumors was evident (range, 1%–20%; mean, 8.9% ± 1.5%), and the percentage of CA-MSCs in each culture was not altered with passaging (up to 10 passages studied; data not shown). To ensure MSC subpopulations isolated from outgrown cultures represented actual MSC populations in human tumors, MSC percentages were compared from freshly isolated CAFs versus cultured CAFs in two different patient tumors. The MSC subpopulation within the CAFs did not significantly change during outgrowth cultures compared with MSC populations from freshly dissociated tumors (Supplementary Fig. S1A and S1B).

A phenotypic hallmark of MSCs is the ability to form colonies and undergo multipotent differentiation. To determine if CAF cells expressing the MSC surface markers possess the functional properties of MSCs, we compared the ability of isolated non-MSC CAF cells

(referred to subsequently in this article as CAF cells) and CA-MSC cells to differentiate into osteoblasts, adipocytes, and chondrocytes in appropriate differentiation media. We found that CA-MSCs successfully demonstrated multipotency, with the ability to differentiate into osteocytes as determined by Alizarin Red staining of calcium deposits, adipocytes as determined by Oil Red O staining of lipid droplets, and chondrocytes as determined by Alcian Blue staining of acidic polysaccharides (Fig. 1E) compared with CAF cells. In addition, CA-MSCs expressed the osteoblast marker RUNX2, the adipocyte marker Adipsin, and the chondrocyte marker cartilage oligomeric matrix protein (COMP; Fig. 1F). We further sorted single MSCs and showed that single CA-MSCs had trilineage potential (Supplementary Fig. S1C). A second characteristic of MSCs is the ability to form colonies (18). When plated at low densities, isolated CA-MSCs successfully formed colonies, whereas the CAFs did not (Fig. 1G and H). These data demonstrate the presence of functional CA-MSCs in human pancreatic cancer samples.

Pancreatic MSCs Promote Tumor Cell Growth and Invasion

To delineate the role of CA-MSCs in pancreatic cancer biology, we first determined the impact of pancreatic CA-MSCs on tumor cell growth and invasion *in vitro.* Coculture of patient-derived UM5 primary PDA cells with CA-MSCs significantly increased proliferation of tumor cells compared with growth medium alone or coculture with CAFs (Supplementary Fig. S2A). To assess the effect of CA-MSCs on tumor cell invasion, GFP-labeled AsPC-1 tumor cells were placed in 3-D type I collagen cultures with the same number of either DsRed-labeled CA-MSC or CAF cells. Under these culture conditions, there was a significant increase in invasion of tumor cells through the collagen matrix when tumor cells were grown with CA-MSCs compared with CAFs or growth medium (*, $P < 0.05$ vs. growth medium or coculture with CAFs; Supplementary Fig. S2B). We next examined whether CA-MSC–mediated proliferation and invasion in tumor cells was due to a secreted factor. The addition of conditioned media from CA-MSCs to primary human PDA cells significantly enhanced their proliferation compared with serum-containing growth media and conditioned media from CAFs (Supplementary Fig. S2A). In addition, there was a significant increase in invasion of tumor cells through the collagen matrix when cultured with conditioned medium from CA-MSC as compared with growth medium (Supplementary Fig. S2B). These data suggest that CA-MSCs produce and secrete factors that promote tumor cell growth and invasion of pancreatic cancer cells.

To determine the impact of CA-MSCs on pancreatic cancer growth and metastasis *in vivo,* we established an orthotopic model system in which either GFP-luciferase–labeled UM5 (KRAS mutant) or GFP-luciferase–labeled BxPC-3 (KRAS wild-type) tumor cells were mixed with the same number of either DsRed-labeled CAF cells or CA-MSC cells, and implanted into the pancreata of NOD-SCID mice. GFP-luciferase– labeled tumor cells, DsRed-labeled CAFs, or CA-MSCs injected in the pancreas alone served as the experimental controls. Implantation of CAFs or CA-MSCs alone did not result in tumor formation (Fig. 2A). Implantation of both UM5 and BxPC-3 tumor cells alone resulted in the development of small tumors comparable in size to those generated by implantation of tumor cells plus CAFs over the 6-week period of study, whereas significantly larger tumors developed in the tumor cells plus CA-MSCs group (Fig. 2A and B; *, $P < 0.01$ compared

with UM5 tumor cells alone and Supplementary Fig. S3A and S3B; *, $P < 0.03$ compared with BxPC-3 tumor cells alone). To determine if coimplantation of tumor cells plus CA-MSCs enhanced tumor growth by promoting tumor cell proliferation *in vivo,* we performed Ki-67 staining. Ki-67 staining was increased in tumors derived from implantation of tumor cells plus CA-MSCs compared with tumors derived from implantation of tumor cells alone or from tumor cells plus CAFs (Fig. 2C). We observed Ki-67 expression was increased in cells expressing CK19, indicating enhanced proliferation of tumor cells. To assess the resultant tumors for the presence of DsRed-labeled CAFs and CA-MSCs, we performed IHC analysis and observed RFP^+ cells in both the tumors derived from implantation of cancer cells and CA-MSCs and cancer cells plus CAFs, showing that these cell populations persisted in the tumors for at least 6 weeks following cell implantation (Fig. 2D). Histologic analysis of the tumors revealed evidence of stromagenesis in all treatment groups, with a significant increase in collagen deposition in the tumor cell plus CA-MSCs group compared with tumor cells alone or the tumor cells plus CAFs group (Fig. 2E and F). These data suggest that CA-MSCs promote tumor growth by enhancing the proliferation of tumor cells. CA-MSCs also induce a more pronounced stromal response which may contribute to pancreatic cancer growth and survival.

MSCs Promote Pancreatic Tumor Cell Metastasis

Initial inspection of the mice in each group revealed the presence of visible metastases only in the tumor cell plus CA-MSCs cohort (Fig. 3A, left). Quantitation of the extent of metastasis by serial sectioning of the livers and lungs of mice in each group revealed metastatic lesions in 4 of 7 mice in the tumor cell plus CA-MSCs group, in 1 of 8 mice in the tumor cell only group, and in 0 of 7 mice in the tumor cell plus CAFs group (Fig. 3A and B; and Supplementary Table S2). For malignant progression to occur, carcinoma cells must traverse through the basement membrane and disseminate into the bloodstream. We next examined the presence and extent of circulating GFP-labeled tumor cells and DsRed-labeled CAFs and CA-MSCs using flow cytometry. Circulating GFP-positive tumor cells were detected in all three groups; however, there was a significant increase in the number of circulating GFP-positive tumor cells in the tumor cells plus CA-MSC group compared with the tumor cells alone and tumor cells plus CAFs groups (Fig. 3C). Further, DsRed-positive circulating cells were detected only in the tumor cells plus CA-MSCs mice and not in the tumor cells plus CAFs mice (Fig. 3D). To determine if CA-MSCs accompany tumor cells to sites of metastasis, we analyzed liver tissue in these animals for the presence of tumor cells (GFP staining) and CA-MSCs (RFP staining). Liver metastases in the tumor cells plus CA-MSCs group contained both GFP-labeled tumor cells and RFP-labeled CA-MSCs cells, with CA-MSCs mainly located next to proliferating tumor cells in the liver (Fig. 3E and F). Both GFP-labeled tumor cells and RFP-labeled MSCs were present adjacent to blood vessels (Fig. 3E and F) in the liver bed. These data suggest that pancreatic CA-MSCs possess the unique ability to travel through the bloodstream and promote tumor cell metastasis.

CA-MSCs Differentially Secrete GM-CSF

Pancreatic cancer is associated with the early development of metastasis, but there is little information on the molecular signals that drive this process. We sought to determine if differential protein secretion might account for functional differences observed between

pancreatic CA-MSCs and CAFs in promoting tumor cell growth, invasion, and metastasis *in vivo.* To ascertain this, we collected conditioned media from cultured CA-MSCs and CAFs (n = 4 patients) and utilized human protein cytokine arrays for analysis (Fig. 4A). We found a number of different cytokines that were significantly upregulated in CA-MSCs compared with CAFs, including GM-CSF, IL6, IL8, and macrophage migration inhibitory factor, whereas others, such as SERPINE1, were expressed in both populations (Supplementary Fig. S4). Of the cytokines differentially expressed in CA-MSCs, GM-CSF was the only cytokine exclusively secreted by the CA-MSCs and not by CAFs in all of the patient samples examined (Fig. 4A; Supplementary Fig. S4), and therefore its role in pancreatic cancer biology was further interrogated.

GM-CSF Receptor Expression in Pancreatic Cancer Cells

Two recent publications have reported that GM-CSF produced by pancreatic tumor cells acts on myeloid-derived suppressor cells to evade immune recognition (19, 20). However, the effect of GM-CSF on the tumor cells themselves was not investigated in these two studies. The biological activities of GM-CSF are exerted through binding to the heteromeric cell surface receptors CSF2Rα and CSF2Rβ. GM-CSF receptors are known to be expressed on neutrophils, monocytes, macrophages, granulocytes, lymphocytes, and endothelial cells (21). Nonhematopoietic tumor cells have also been shown to express the receptors and respond to GM-CSF (22). To determine the potential role of GM-CSF on cancer cell function, we first examined expression of the GM-CSF receptor proteins CSF2Rα and CSF2Rβ on five different primary human pancreatic cancer cell lines. The GM-CSF receptors CSF2Rα and CSF2Rβ were expressed in four of five primary carcinoma cell lines tested (Supplementary Fig. S5). Expression of both GM-CSF receptors was verified within human PDA tissue sections, with colocalization of both CSF2Rα and CSF2Rβ receptor expression (Fig. 4B–D). We found GM-CSF receptor expression in cells coexpressing CK19 within PDA tissue sections (Fig. 4B–D). Expression of the GM-CSF receptor proteins was also evident in CD45-positive immune cells in the stroma (Fig. 4B–D). In contrast, Western blot analysis showed lack of GM-CSF receptor expression by CAF cells (Fig. 4E). These results support the notion that tumor cells may have the ability to respond to GM-CSF. Pancreatic tumor cells have also been reported to produce GM-CSF, and it has been shown that mutations in KRAS increase the expression of GM-CSF in tumor cells (19–20). We next measured the amount of GM-CSF produced by tumor cells and tumor cells cultured with CA-MSCs. CFPAC-1 and UM2 cells with KRAS mutations secreted significantly higher amounts of GM-CSF compared with KRAS wild-type BxPC-3 cells (Fig. 4F). Interestingly, we found a significant increase in GM-CSF secretion when either KRAS wild-type or mutant KRAS tumor cells were cultured with CA-MSCs (Fig. 4F) compared with when the tumor cells were cultured alone. This increase in GM-CSF secretion could be a result of increased GM-CSF secretion from either tumor cells, MSCs, or both when the cells are cocultured.

MSC-Derived GM-CSF Is Required for Pancreatic Cancer Cell Invasion and Transendothelial Migration

To understand the role of MSC-derived GM-CSF on pancreatic cancer cell function, we either knocked down GM-CSF in CA-MSCs or knocked down the expression of the GM-CSF receptor CSFR2α in two different primary tumor cells (UM5, UM8) using two

different siRNA constructs targeting different portions of the molecule (Fig. 5A and B). A significant increase in the number of GFP-labeled tumor cells was observed when they were cocultured with control CA-MSC cells compared with tumor cells alone, and this increase was abrogated in tumor cells cocultured with CA-MSCs expressing GM-CSF shRNA (Fig. 5C and D). Furthermore, as shown in Fig. 5C and D, the ability of MSCs to induce tumor cell proliferation in two different primary cell lines (UM5, UM8) was abolished when the tumor cells had knockdown of the GM-CSF receptor, suggesting that MSC-induced tumor cell proliferation is dependent on an intact GM-CSF signaling pathway in tumor cells. To examine the effect of GM-CSF produced by CA-MSCs on tumor cell invasion, GFP-labeled UM5 tumor cells were embedded in a 3-D type I collagen matrix, either alone or with DsRed-labeled CA-MSCs. GFP-labeled tumor cells alone were incapable of invading into surrounding type I collagen for the 5 days of study (Fig. 5E, left), whereas tumor cells cocultured with CA-MSCs expressing control shRNA demonstrated invasion of both red CA-MSCs and green tumor cells into the collagen (Fig. 5E). When tumor cells were mixed with CA-MSCs expressing GM-CSF shRNA, the ability of tumor cells to invade through collagen was completely inhibited despite the ability of the MSCs expressing GM-CSF shRNA themselves to exhibit a limited amount of invasion (Fig. 5E and F). To verify the specific role of GM-CSF in this process, we added exogenous GM-CSF and were able to reverse the inhibition of tumor cell invasion with GM-CSF shRNA CA-MSC cells to control shRNA levels. (Fig. 5E, right plot and Fig. 5F). These findings clearly demonstrate that CA-MSC–derived GM-CSF promotes tumor cell proliferation and invasion through type I collagen.

In earlier experiments, we observed that CA-MSCs promoted the ability of tumor cells to metastasize, with increased numbers of tumor cells present in the bloodstream (Fig. 3C). To examine if CA-MSC–derived GM-CSF might be responsible for the increased number of circulating tumor cells seen in the CA-MSCs plus tumor cell group, we examined the effect of GM-CSF knockdown in CA-MSCs on tumor cell transendothelial migration. Tumor cells alone or in combination with either CA-MSCs expressing control shRNA or GM-CSF shRNA were plated on a monolayer of human umbilical vascular endothelial cells, and the ability of tumor cells to migrate through the endothelial cell layer was measured. Tumor cells cocultured with CA-MSCs expressing control shRNA readily invaded through the endothelial layer, whereas this ability was significantly diminished in tumor cells cocultured with CA-MSCs with GM-CSF knockdown (Fig. 5G and H).

GM-CSF Induces EMT and Stemness in Tumor Cells

One of the mechanisms by which epithelial tumor cells migrate and invade is by undergoing EMT, a complex reprogramming event in which epithelial cells lose polarity and change to an invasive, mesenchymal phenotype. To understand the mechanism by which GM-CSF produced by CA-MSCs induces invasion in tumor cells, we treated tumor cells with recombinant GM-CSF and assessed changes in markers of EMT. Treatment with recombinant GM-CSF downregulated the expression of the epithelial marker E-cadherin and induced expression of the EMT markers TWIST1 and vimentin in 3 different primary PDA lines (Fig. 6A and B). Both CSF2Rα and CSF2Rβ GM-CSF receptors are known to transduce signals through the JAK–STAT signaling pathway (23). To determine if GM-CSF–

induced changes in EMT-related genes utilize the JAK–STAT signaling pathway in CA-MSCs, we treated three primary PDA lines (UM5, UM2, and UM8) with GM-CSF and noted induction of phosphorylation of STAT3 in all three lines tested (Fig. 6B). Further, knockdown of STAT3 in UM5 tumor cells using two different siRNAs blocked the ability of GM-CSF to induce EMT markers (Fig. 6C).

It has been reported that there is a direct link between EMT and gain of CSC properties (24). The ability to form spheroids in suspension is an attribute generally associated with stem cell–like properties. To determine if CA-MSCs effected stemness of tumor cells, GFP-labeled tumor cells were either cocultured with CA-MSCs or CAFs, or treated with conditioned media from CA-MSCs or CAFs and sphere assays were performed. Exposure of PDA cells to CA-MSCs promoted tumor sphere formation to a significantly greater extent over control and CAFs (Supplementary Fig. S6). We next tested to see if GM-CSF could mimic the effects of CA-MSCs in inducing stemness in tumor cells. Sphere-forming assays were performed using three different tumor cell lines (UM2, UM5, and UM8) cultured in growth media with or without recombinant GM-CSF. Treatment with GM-CSF significantly promoted tumor sphere formation (Fig. 6D). Further, GM-CSF treatment significantly increased the percentage of CSCs measured using the established markers ESA^{+}, $CD44^{+}$, and $CD24^{+}$ (25) in all three primary PDA cell lines (Fig. 6E). To determine if GM-CSF might have a preferential effect on the CSC population, we measured receptor expression in CSCs versus bulk tumor cells. The primary PDA cell lines demonstrated heterogeneity in the GM-CSF receptor expression; however, in each the CSC population expressed significantly higher levels of GM-CSF receptor than the bulk tumor cell population (Fig. 6F), suggesting there may be enhanced GM-CSF signaling in the CSC population within tumors.

GM-CSF Is Required for Pancreatic Cancer MSC-Induced Tumor Metastasis

Based on our *in vitro* data, we hypothesized that GM-CSF from CA-MSCs might drive tumor cell growth and metastasis *in vivo.* To test this hypothesis, 10^4 GFP-luciferase–labeled UM5 primary pancreatic tumor cells alone or in combination with the same number of DsRed-labeled CA-MSCs expressing control shRNA or GM-CSF shRNA were orthotopically implanted into the pancreata of NOD-SCID mice. Animals with tumor cells implanted with CA-MSC cells expressing control shRNA developed tumors with a significant increase in luciferase activity as compared with animals implanted with tumor cells alone (Fig. 7A and B). This increase in tumor growth was inhibited when tumor cells were instead coimplanted with CA-MSCs expressing GM-CSF shRNA (Fig. 7A and B). In addition, the ability of CA-MSCs expressing control shRNA to enhance tumor cell metastasis was completely blocked when tumor cells were coimplanted with CA-MSCs with GM-CSF knockdown (Fig. 7C). These data suggest that GM-CSF expression in CA-MSCs plays a critical role in pancreatic cancer growth and metastasis *in vivo.* As GM-CSF has been previously shown to play a critical role in the immune modulation of pancreatic cancer (19–20), we next determined if CA-MSCs drive monocyte to macrophage polarization and polarization of macrophages to an $ARG1^{+}$ phenotype. We examined for F4/80- and ARG1-expressing cells in the CA-MSCs expressing GM-CSF shRNA tumors and CA-MSC expressing control shRNA tumors to determine if there were differences in the presence of tumor-associated macrophages (TAM). We found significantly fewer F4/80-expressing and

ARG1-expressing cells in tumors derived from CA-MSCs expressing GM-CSF shRNA compared with the CA-MSC control shRNA tumors (Supplementary Fig. S7A and S7B), suggesting that GM-CSF plays a role in the recruitment and polarization of TAMs in the tumor microenvironment. These results are consistent with a recent report demonstrating a role for CA-MSCs in regulating macrophage polarization (26).

DISCUSSION

A defining feature of pancreatic adenocarcinoma is a profound desmoplastic response, but the heterogeneity of stromal cells and their functional contribution remains unknown. PDA stroma is generally believed to be tumor promoting (3, 6, 7, 27, 28). However, two recent studies suggested that eliminating stroma by targeted deletion results in aggressive tumors and concluded that activated stroma is beneficial and not harmful (9, 10). As new therapeutic avenues targeting different components of the tumor stroma are being investigated, it becomes important to understand stromal heterogeneity and the contribution of its individual components to tumorigenesis.

CAFs are a heterogeneous mesenchymal cell population found in the stroma of many tumors, but how they contribute to tumorigenesis is incompletely understood. In this study, we demonstrate the presence of cancer-associated MSCs within the human PDA tumor microenvironment. These CA-MSCs had a normal morphologic appearance, possessed markers ascribed to previously defined MSC populations, and possessed the capacity to differentiate into adipose, cartilage, and bone under appropriate culture conditions. CA-MSCs lacked the KRAS mutations present in their matching neoplastic epithelial cells from the same patient tumors. These pancreatic CA-MSCs promoted tumor cell growth, invasion, transendothelial migration, and subsequently tumor cell metastasis via secretion of GM-CSF, establishing a novel role for this subpopulation of CAFs in pancreatic cancer.

Interestingly, a previous study suggested that CAFs might represent a heterogeneous population of stromal cells in human PDA. The authors identified a subset of pancreatic CAFs, CD10-expressing stellate cells, which induced an invasive phenotype in pancreatic cancer cells more extensively than cells lacking CD10 expression (4). However, the mechanism by which CD10 stellate cells enhanced tumorigenesis was not defined. To determine if the CA-MSC cell population overlapped with the previously defined CD10-expressing stellate cells, we examined CD10 expression in CA-MSCs and found that only a small subset of CA-MSCs also express CD10 (Supplementary Table S3). This suggests that CAFs are heterogeneous, and multiple different subpopulations may exist with distinct/overlapping roles.

Interestingly, we observed that human pancreatic CA-MSCs traveled from the primary injection site, entered the bloodstream, and accompanied tumor cells to distant metastatic sites, a behavior that was not observed in CAFs. This ability of pancreatic stromal cells to accompany cancer cells to metastatic sites is consistent with an earlier report examining the function of human pancreatic stellate cells (hPSCs), which are quiescent and express vitamin A droplets in the normal adult pancreas but become activated myofibroblasts in the tumor microenvironment of PDA. In a sex mismatch study using male hPSCs injected with female

cancer cells into the pancreas of female mice, Y chromosome–positive stellate cells were detected at metastatic sites, suggesting hPSCs accompany cancer cells on their metastatic journey (6). The relationship between CA-MSCs and hPSCs is currently unknown. In the context of our study, it is possible that CA-MSCs provide an integral role in interacting with cancer cells in detaching from the primary tumor and traveling to distant sites. Another possibility is that CA-MSCs travel to metastatic sites and establish a microenvironment that would facilitate cancer cell seeding and growth.

It has been increasingly appreciated that metastatic traits can be acquired through exposure of neoplastic epithelial cells to paracrine signals from stromal cells in the tumor microenvironment. We observed a number of cytokines, including GM-CSF, IL6, IL8, GRO, and MIF, to be more highly expressed by the CA-MSCs compared with the CAFs. Interestingly, only GM-CSF was exclusively expressed by CA-MSC cells compared with CAFs. GM-CSF has been reported previously to have elevated expression in ovarian and lung CA-MSCs compared with normal MSCs (12, 29). This makes GM-CSF an attractive therapeutic target, and understanding its role might have broader implications beyond pancreatic cancer to other cancer types where CA-MSCs have been shown to play a role in tumorigenesis. It has previously been reported that CA-MSCs (12, 13) and bone marrow MSCs (30) endow tumor cells with invasive and metastatic properties and thereby expedite tumor metastasis. Here, we demonstrate that CA-MSCs produce a complex mixture of cytokines, including GM-CSF, which promote pancreatic tumor growth and metastasis. A central finding of our study is that GM-CSF induces EMT and expression of CSC markers in tumor cells. It is believed that signaling pathways regulating EMT convey stem cell phenotypes to neoplastic cells, accounting for their ability to metastasize. It is proposed, based on MetaCore analysis, that GM-CSF maintains a stem cell pool in solid cancers via activation of SLUG, SNAIL1, or TWIST1 (31–33). These findings suggest that a major contribution of the MSC subpopulation to tumorigenesis is their ability to produce extracellular signals which promote growth, stemness, and metastasis. Furthermore, targeting these cytokine-driven signaling pathways may represent a novel therapeutic approach for a disease with few treatment options.

Our study reinforces the heterogeneity seen within the human CAFs and suggests a role for CA-MSCs in promoting pancreatic cancer growth and metastasis. The identification of CA-MSCs in primary pancreatic tumors in patients allows for a better understanding of the role of CA-MSCs in pancreatic tumorigenesis. Our data suggest that a mechanism by which CA-MSCs enhance tumor cell metastasis *in vivo* is through the production of GM-CSF. Our data highlight a critical new role of GM-CSF in mediating mesenchymal–epithelial crosstalk in pancreatic cancer, and suggest that targeting GM-CSF may abrogate the ability of CA-MSCs within the pancreatic tumor microenvironment to promote pancreatic cancer growth and metastasis and warrant further investigation as a therapeutic strategy for patients. These data further highlight that studies to define the metastatic properties of cancer cells may need to focus on proteins that confer responsiveness of primary tumor cells to stromal signals. In light of these data, ongoing trials with GM-CSF secreting oncolytic viral and vaccine therapies in PDA should be considered with prudence.

METHODS

Primary Human Pancreatic Cancer and CAF Cell Lines

All human pancreatic cancer samples were provided by the Tissue Procurement Core at University of Michigan using Institutional Review Board (IRB) guidelines from patients who underwent surgical resection at University of Michigan Hospital. The UM2, UM3, UM5, UM8, UM15, UM16, UM18, and UM19 primary human pancreatic cancer cell lines were generated in our laboratory and were cultured in RPMI-1640 supplemented with 10% heat-inactivated FBS, 2 mmol/L L-glutamine, 100 units/mL penicillin, 100 μg/mL streptomycin (Invitrogen) in 95% air and 5% carbon dioxide at 37°C. The UM18, UM19, UM27, UM35, UM39, UM73, UM85, UM86, UM87, UM89, UM90, UM93, UM95, UM99, UM113,15-1405, and 15-1409 human pancreatic CAF cell lines were created at University of Michigan under IRB guidelines from primary patient pancreatic adenocarcinomas using a previously described outgrowth technique (12). No further authentication was carried out on these cell lines.

Constructs

Lentiviral constructs expressing control shRNA (RHS4743) or shRNAs 1 and 2 targeting human GM-CSF (RHS4696-99706997 or RHS4696-99709227) were purchased from Dharmacon, Inc. Non-targeting control siRNAs and siRNA for STAT3 and CSFR2A were purchased from Dharmacon.

Flow Cytometry

Single-cell suspensions of CAFs or dissociated single cells from pancreatic tumors were transferred to 5 mL tubes, washed with Hank's Balanced Salt Solution (HBSS)/2% FBS twice, and resuspended in HBSS/2% FBS at a concentration of 10^6 cells per 100 μL. The following antibodies were added for flow cytometric analysis of CAF cells for MSC markers: anti–CD90-biotin (1:50; BD Pharmingen; Cat#555594), streptavidin APC-cy7 (1:100; BD Pharmingen; Cat#554063), anti–CD73-FITC (1:50; BD Pharmigen; clone: AD2, Cat#561254), anti–CD44-PE (1:50; BD Pharmingen; Cat#550989), anti–CD49α-APC (1:50; RD; Cat#FAB5676A). Other antibodies used included biotin-conjugated mouse IgG1, K Isotype control (1:50; eBioscience; clone: P3, Cat# 13-4714-B5), anti–c-Met-biotin (1:50; eBioscience; clone: eBioclone 97 Cat#13-8858-80), Streptavidin APC (1:100; BD Pharmingen; Cat#554067), PE-conjugated Mouse IgG1, K Isotype control (1:50; eBioscience; clone: P3, Cat#12-4714-41), FITC-conjugated mouse IgG1 (1:50; Becton Dickinson; Cat#340755). For the outgrowth validation study, the tumor tissue and the cultured CAF sample was first gated on FAP-positive cells (anti-FAP antibody; R&D systems; Cat#AF3715). Enumeration of CSCs using ESA, CD44, and CD24 antibodies was performed as previously described (25). Enumeration for CSF2RA expression was done using Anti-CSFR2α antibody (Santa Cruz Biotechnology). Data analysis was performed using Summit V6.2 (Beckman Coulter, Inc.).

MSC Differentiation Assays

Cells were plated at a density of 5×10^4 cells/well in 6-well plates (Falcon), and assays were performed following the specific instructions of commercially available differentiation kits (GIBCO) for osteogenesis, chondrogenesis, and adipogenesis.

MSC Colony-Forming Assays

Flow-sorted CA-MSCs and CAFs were plated at 100 cells per 100-mm tissue culture dish (Falcon) in complete culture medium (Minimum Essential Medium) with 20% FBS. Cells were incubated for 10 to 14 days at 37°C in 5% humidified CO_2, then washed with PBS, and stained with Gram's crystal violet solution (Fluke) for 5 minutes at room temperature. The plates were washed with PBS, and visible colonies were counted.

KRAS Mutation Assays

RNA was extracted from primary tumor cells and matching CAFs using the RNeasy micro kit (Qiagen). cDNA was generated by reverse transcription of total RNA using the high-capacity cDNA reverse transcription kit (AB applied biosystems). cDNA was amplified for *KRAS* using forward: 5′-GCAGTGGCGGCGGCGAAGGT-3′; reverse: 5′-ATGGCAAATACACAAAGAAAG-3′ KRAS primers. Size was confirmed by gel electrophoresis, and the PCR product was excised from gel and purified using a PCR purification kit (QIAquick). Samples were submitted for sequencing to the University of Michigan Sequencing Core. Mutations in codon 12/13 and codon 61 were analyzed.

In Vivo Tumorigenicity Assays

Six-week-old NOD/SCID mice (Taconic) were housed under pathogen-free conditions. Animal experiments were approved by the University of Michigan Animal Care and Use Committee and were performed in accordance with their established guidelines. Mice were anesthetized with an i.p. injection of xylazine (9 mg/kg) and ketamine (100 mg/kg). A median laparotomy was performed, and 1×10^4 primary human pancreatic cells (UM5) or 1×10^5 BxPC-3 cells infected with a lentivirus encoding GFP-luciferase (University of Michigan Vector Core) alone or with an equal number of either DsRed-labeled CAF or CA-MSC cells were injected into the pancreatic tail using a 30-gauge needle ($n = 8$ per group for UM5 and $n = 4$ for BxPC-3). For experiments addressing the role of GM-CSF in tumorigenesis, 1×10^4 UM5 cells infected with a lentivirus encoding GFP-luciferase alone or with a similar number of either CA-MSC cells expressing control shRNA or GM-CSF shRNA-2 were injected into the pancreatic tail using a 30-gauge needle ($n = 8$ per group). To prevent leak at the injection site, the needle was slowly withdrawn and a sterile cotton swab was applied to the injection site for 30 seconds. Bioluminescent imaging of the mice was performed weekly using a Xenogen IVIS 200 imaging system (Xenogen Biosciences). Six to 8 weeks following cell injections, mice were euthanized with CO_2 inhalation and tissue processed to assess the extent of primary tumor growth and metastasis. To screen for the presence of metastasis, serial sections of the entire liver and lung were taken every 10 μm of mice in each group. Blood was collected for flow cytometric analysis of circulating GFP-labeled tumor cells and DsRed-labeled CAF and CA-MSC enumeration. Blood samples were subjected to negative selection of leukocytes and erythrocytes using FACS lysis buffer

(BD). The enriched cells were then resuspended in 2% FBS-HBSS buffer for further flow cytometric analysis.

Human Cytokine Array Assays

A total of 1×10^4 CA-MSC and CAF cells were plated in 10-cm dishes with RPMI supplemented with 10% FBS. After 2 days, the conditioned media were collected and centrifuged at 1,200 rpm for 5 minutes, and cytokine levels were measured using human cytokine array kits (R&D Systems) according to the manufacturer's directions.

ELISA Assays

Conditioned media were collected from 1×10^4 CA-MSC, tumor cells, and tumor cells cultured with CA-MSCs (1:1), and GM-CSF levels were measured using the human GM-CSF ELISA kit (R&D Systems) according to the manufacturer's directions.

3-D Invasion Assays

Cells were plated in collagen (see Supplementary Methods). After the collagen was solidified, 500 μL of growth media or conditioned media from CAFs or CA-MSCs was added to each well. For experiments examining the role of GM-CSF in cell invasion, tumor cells alone or tumor cells with control shRNA CA-MSCs or GM-CSF shRNA CA-MSCs (1:1) were used. After the collagen was solidified, 500 μL of growth media was added to each well, and 500 μL of growth media with GM-CSF (100 ng/mL) was added to one of the wells containing tumor cells and GM-CSF-shRNA CA-MSCs. Stitched images were taken with the Nikon confocal microscope every day for 5 days, and invasion outside of the collagen droplet was measured with ImageJ software.

Transendothelial Migration Assays

Transendothelial migration assays using transendothelial migration assay kits (Cell Biolabs) were performed according to the manufacturer's directions (Supplementary Methods).

Tumorsphere-Forming Assays

AsPC-1 (ATCC) or primary human pancreatic cancer cells ($1 \times 10^{4)}$ were plated in ultralow-adherence plates (Corning; 3471) in Schwann Cell Medium (Supplementary Methods). Cells were passaged after 2 weeks into fresh media. Tumorspheres were recognized as three-dimensional cell colonies.

Statistical Analyses

All statistical analyses of flow cytometry, luciferase signal intensity IHC quantifications, and pathologic scores were determined by Student *t* test and one-way ANOVA using GraphPad Prism (GraphPad Software). Quantification of distance of invasion and size of spheres was done using ImageJ analysis. Statistical significance was accepted if $P < 0.05$.

Supplementary Material

Refer to Web version on PubMed Central for supplementary material.

Acknowledgments

The authors thank past and present members of the Simeone laboratory for helpful discussions, Dr. Mark J. Hoenerhoff from the University of Michigan ULAM Pathology Core for assistance in enumeration of metastases from tissue slides, and Martin White and Michael Dellheim for assisting with flow cytometry analysis. They also appreciate the assistance of the University of Michigan Histopathology Core, Mouse Imaging Core, and DNA Sequencing Core.

Grant Support

This research was supported by the 2014 Pancreatic Cancer Action Network-AACR Innovative Grant, Grant Number 14-60-25-SIME, and the Rogel Family Pancreatic Cancer Gift Fund.

References

1. Chen J, Carcamo JM, Borquez-Ojeda O, Erdjument-Bromage H, Tempst P, Golde DW. The laminin receptor modulates granulocyte-macrophage colony-stimulating factor receptor complex formation and modulates its signaling. Proc Natl Acad Sci U S A. 2003; 100:14000–5. [PubMed: 14614142]
2. Olive KP, Jacobetz MA, Davidson CJ, Gopinathan A, McIntyre D, Honess D, et al. Inhibition of Hedgehog signaling enhances delivery of chemotherapy in a mouse model of pancreatic cancer. Science. 2009; 324:1457–61. [PubMed: 19460966]
3. Hwang RF, Moore T, Arumugam T, Ramachandran V, Amos KD, Rivera A, et al. Cancer-associated stromal fibroblasts promote pancreatic tumor progression. Cancer Res. 2008; 68:918–26. [PubMed: 18245495]
4. Ikenaga N, Ohuchida K, Mizumoto K, Cui L, Kayashima T, Morimatsu K, et al. CD10+ pancreatic stellate cells enhance the progression of pancreatic cancer. Gastroenterology. 2010; 139:1041–51. 51 e1–8. [PubMed: 20685603]
5. Kikuta K, Masamune A, Watanabe T, Ariga H, Itoh H, Hamada S, et al. Pancreatic stellate cells promote epithelial-mesenchymal transition in pancreatic cancer cells. Biochem Biophys Res Commun. 2010; 403:380–4. [PubMed: 21081113]
6. Xu Z, Vonlaufen A, Phillips PA, Fiala-Beer E, Zhang X, Yang L, et al. Role of pancreatic stellate cells in pancreatic cancer metastasis. Am J Pathol. 2010; 177:2585–96. [PubMed: 20934972]
7. Erkan M, Michalski CW, Rieder S, Reiser-Erkan C, Abiatari I, Kolb A, et al. The activated stroma index is a novel and independent prognostic marker in pancreatic ductal adenocarcinoma. Clin Gastroenterol Hepatol. 2008; 6:1155–61. [PubMed: 18639493]
8. Fujita H, Ohuchida K, Mizumoto K, Nakata K, Yu J, Kayashima T, et al. alpha-Smooth muscle actin expressing stroma promotes an aggressive tumor biology in pancreatic ductal adenocarcinoma. Pancreas. 2010; 39:1254–62.
9. Ozdemir BC, Pentcheva-Hoang T, Carstens JL, Zheng X, Wu CC, Simpson TR, et al. Depletion of carcinoma-associated fibroblasts and fibrosis induces immunosuppression and accelerates pancreas cancer with reduced survival. Cancer Cell. 2014; 25:719–34. [PubMed: 24856586]
10. Rhim AD, Oberstein PE, Thomas DH, Mirek ET, Palermo CF, Sastra SA, et al. Stromal elements act to restrain, rather than support, pancreatic ductal adenocarcinoma. Cancer Cell. 2014; 25:735–47. [PubMed: 24856585]
11. Cao H, Xu W, Qian H, Zhu W, Yan Y, Zhou H, et al. Mesenchymal stem cell-like cells derived from human gastric cancer tissues. Cancer Lett. 2009; 274:61–71. [PubMed: 18849111]
12. McLean K, Gong Y, Choi Y, Deng N, Yang K, Bai S, et al. Human ovarian carcinoma-associated mesenchymal stem cells regulate cancer stem cells and tumorigenesis via altered BMP production. J Clin Invest. 2011; 121:3206–19. [PubMed: 21737876]
13. Lin JT, Wang JY, Chen MK, Chen HC, Chang TH, Su BW, et al. Colon cancer mesenchymal stem cells modulate the tumorigenicity of colon cancer through interleukin 6. Exp Cell Res. 2013; 319:2216–29. [PubMed: 23751564]
14. Rhim AD, Mirek ET, Aiello NM, Maitra A, Bailey JM, McAllister F, et al. EMT and dissemination precede pancreatic tumor formation. Cell. 2012; 148:349–61. [PubMed: 22265420]

15. Seeberger KL, Dufour JM, Shapiro AM, Lakey JR, Rajotte RV, Korbutt GS. Expansion of mesenchymal stem cells from human pancreatic ductal epithelium. Lab Invest. 2006; 86:141–53. [PubMed: 16402034]
16. Crisan M, Yap S, Casteilla L, Chen CW, Corselli M, Park TS, et al. A perivascular origin for mesenchymal stem cells in multiple human organs. Cell Stem Cell. 2008; 3:301–13. [PubMed: 18786417]
17. Dominici M, Le Blanc K, Mueller I, Slaper-Cortenbach I, Marini F, Krause D, et al. Minimal criteria for defining multipotent mesenchymal stromal cells. The International Society for Cellular Therapy position statement. Cytotherapy. 2006; 8:315–7. [PubMed: 16923606]
18. Prockop DJ, Phinney DG, Bunnell BA. Methods and protocols. Preface. Methods Mol Biol. 2008; 449:v–vii. [PubMed: 18453071]
19. Bayne LJ, Beatty GL, Jhala N, Clark CE, Rhim AD, Stanger BZ, et al. Tumor-derived granulocyte-macrophage colony-stimulating factor regulates myeloid inflammation and T cell immunity in pancreatic cancer. Cancer Cell. 2012; 21:822–35. [PubMed: 22698406]
20. Pylayeva-Gupta Y, Lee KE, Hajdu CH, Miller G, Bar-Sagi D. Oncogenic Kras-induced GM-CSF production promotes the development of pancreatic neoplasia. Cancer Cell. 2012; 21:836–47. [PubMed: 22698407]
21. Hercus TR, Thomas D, Guthridge MA, Ekert PG, King-Scott J, Parker MW, et al. The granulocyte-macrophage colony-stimulating factor receptor: Linking its structure to cell signaling and its role in disease. Blood. 2009; 114:1289–98. [PubMed: 19436055]
22. Baldwin GC, Gasson JC, Kaufman SE, Quan SG, Williams RE, Avalos BR, et al. Nonhematopoietic tumor cells express functional GM-CSF receptors. Blood. 1989; 73:1033–7. [PubMed: 2537665]
23. Martinez-Moczygemba M, Huston DP. Biology of common beta receptor-signaling cytokines: IL-3, IL-5, and GM-CSF. J Allergy Clini Immunol. 2003; 112:653–65. quiz 66.
24. Mani SA, Guo W, Liao MJ, Eaton EN, Ayyanan A, Zhou AY, et al. The epithelial-mesenchymal transition generates cells with properties of stem cells. Cell. 2008; 133:704–15. [PubMed: 18485877]
25. Li C, Heidt DG, Dalerba P, Burant CF, Zhang L, Adsay V, et al. Identification of pancreatic cancer stem cells. Cancer Res. 2007; 67:1030–7. [PubMed: 17283135]
26. Mathew E, Brannon AL, Del Vecchio A, Garcia PE, Penny MK, Kane KT, et al. Mesenchymal stem cells promote pancreatic tumor growth by inducing alternative polarization of macrophages. Neoplasia. 2016; 18:142–51. [PubMed: 26992915]
27. Lonardo E, Frias-Aldeguer J, Hermann PC, Heeschen C. Pancreatic stellate cells form a niche for cancer stem cells and promote their self-renewal and invasiveness. Cell Cycle. 2012; 11:1282–90. [PubMed: 22421149]
28. Hamada S, Masamune A, Takikawa T, Suzuki N, Kikuta K, Hirota M, et al. Pancreatic stellate cells enhance stem cell-like phenotypes in pancreatic cancer cells. Biochem Biophys Res Commun. 2012; 421:349–54. [PubMed: 22510406]
29. Hofer EL, Labovsky V, La Russa V, Vallone VF, Honegger AE, Belloc CG, et al. Mesenchymal stromal cells, colony-forming unit fibroblasts, from bone marrow of untreated advanced breast and lung cancer patients suppress fibroblast colony formation from healthy marrow. Stem Cells Dev. 2010; 19:359–70. [PubMed: 19388812]
30. Karnoub AE, Dash AB, Vo AP, Sullivan A, Brooks MW, Bell GW, et al. Mesenchymal stem cells within tumour stroma promote breast cancer metastasis. Nature. 2007; 449:557–63. [PubMed: 17914389]
31. Banerjee A, Qian P, Wu ZS, Ren X, Steiner M, Bougen NM, et al. Artemin stimulates radio- and chemo-resistance by promoting TWIST1-BCL-2-dependent cancer stem cell-like behavior in mammary carcinoma cells. J Biol Chem. 2012; 287:42502–15. [PubMed: 23095743]
32. Levina V, Marrangoni AM, DeMarco R, Gorelik E, Lokshin AE. Drug-selected human lung cancer stem cells: cytokine network, tumorigenic and metastatic properties. Plos One. 2008; 3:e3077. [PubMed: 18728788]
33. Aliper AM, Frieden-Korovkina VP, Buzdin A, Roumiantsev SA, Zhavoronkov A. A role for G-CSF and GM-CSF in nonmyeloid cancers. Cancer Med. 2014; 3:737–46. [PubMed: 24692240]

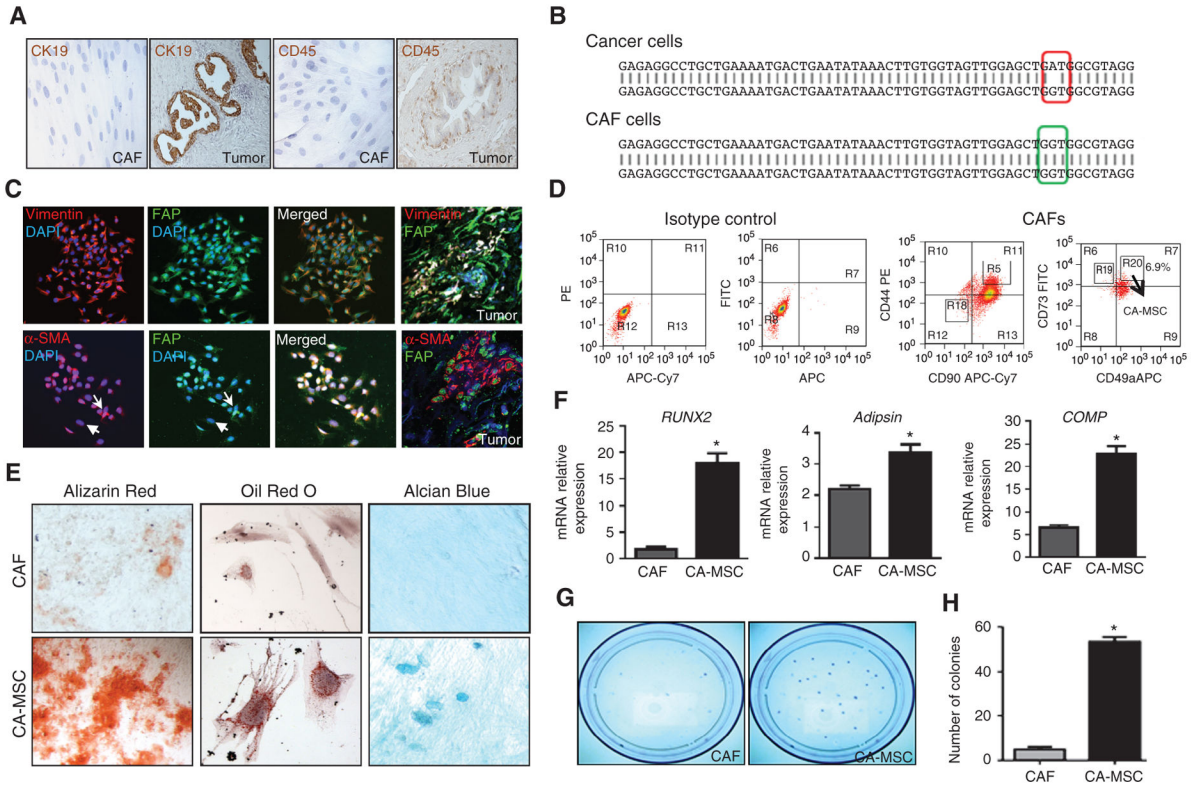

Figure 1.

Isolation of primary human pancreatic cancer-associated MSCs (CA-MSC). **A,** IHC staining for CK19 and CD45 protein expression in representative samples of human pancreatic cancer tissue and isolated CAF cells. **B,** representative KRAS mutational analysis of matched cancer cells and isolated CAFs. A mutation is present in the codon 12/13 region (red) in the cancer cells but absent in the CAFs (green). **C,** immunofluorescence staining for α-SMA (red), vimentin (red), and FAP (green) protein in human pancreatic cancer tissue and isolated CAFs. Arrows indicate higher expression of protein within cells, and arrowheads indicate lower expression of protein within cells. Magnification, ×200. **D,** FACS analysis of primary human pancreatic CAF line, demonstrating $CD44^+$ $CD73^+$ $CD90^+$ $CD49\alpha^+$ expression. **E,** CA-MSCs but not CAFs demonstrate multipotent differentiation capacity in differential culture conditions. Specific cell stains used were Alizarin Red for bone, Oil Red O for adipose, and Alcian Blue for cartilage. Magnification, ×200. **F,** quantitative RT-PCR analysis of the differentiation-specific expression markers *RUNX2* for bone, *Adipsin* for adipose, and *COMP* for cartilage. All samples were normalized to GAPDH; $n = 3$; *, $P < 0.05$. **G,** photograph of colonies stained with crystal violet. **H,** quantitation of colonies generated from CAF vs. CA-MSC is shown; $n = 3$; *, $P < 0.05$ vs. CAF.

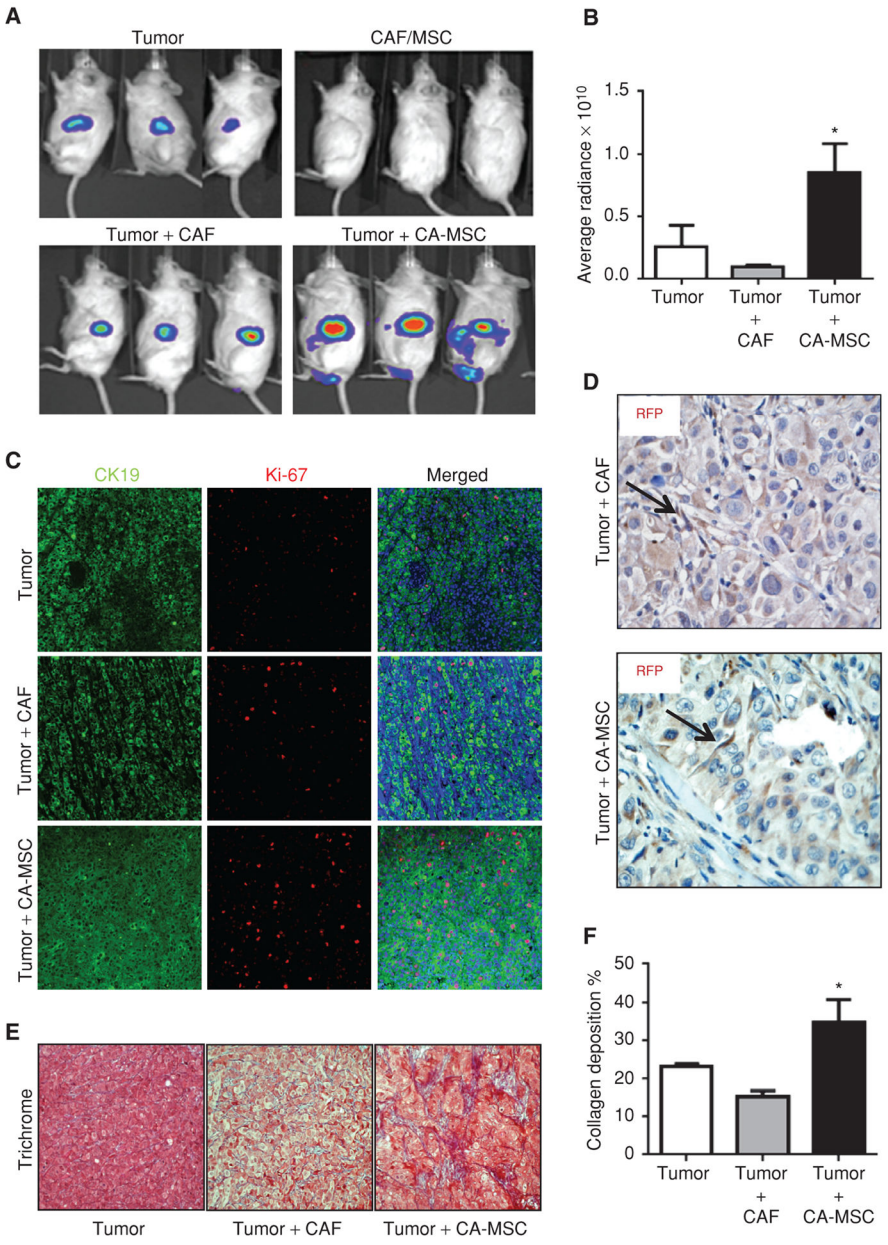

Figure 2.

Pancreatic CA-MSCs promote tumor growth and metastasis. 10^4 UM5 pancreatic cancer cells transduced with a luciferase-expressing lentivirus were orthotopically injected alone or with CAF or CA-MSC into the pancreatic tail of NOD/SCID mice ($n = 8$ per group). **A,** representative bioluminescent images of animals in each group are shown at 3 weeks after injection depicting tumor growth. **B,** bioluminescent-based tumor growth (measured by signal intensity p/s/cm$^{2)}$ of luciferase tumors alone or in combination with CAFs or CA-MSCs (MSC). Pooled results of the average tumor size ± SEM from each group. *, $P < 0.05$. **C,** sections from orthotopic pancreatic tumors were stained for CK19 (green) to mark epithelial cells and Ki-67 (red) to mark proliferating cells. Nuclei were stained with DAPI (blue). **D,** immunostaining for RFP on sections of tumor + CAF and tumor + CA-MSC

orthotopic grafts at 6 weeks after implantation. **E,** trichrome blue staining showing differences in fibrosis in different groups. **F,** quantitation of % collagen-positive area over total visual field (20x, $n = 5$) is shown (*, $P < 0.05$ vs. tumor).

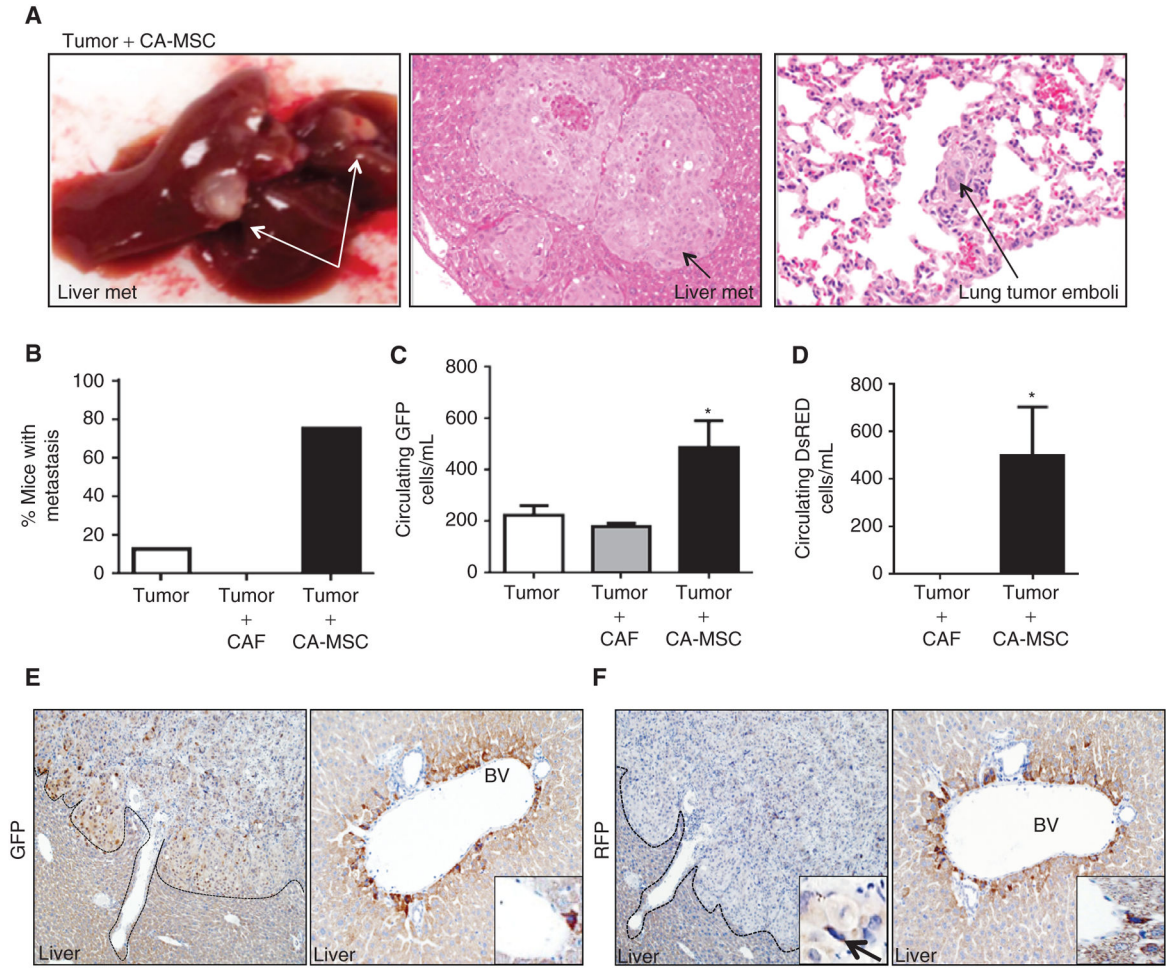

Figure 3.

Pancreatic CA-MSCs promote tumor cell metastasis. Pancreatic cancer cells transduced with a luciferase-expressing lentivirus were orthotopically injected alone or with CAFs or CA-MSCs into the pancreatic tail of NOD/SCID mice ($n = 8$ per group). **A,** representative images of gross metastatic lesions in the liver from mice in the tumor + CA-MSCs groups at 6 weeks after implantation, and representative hematoxylin and eosin–stained sections of metastatic nodules in liver and lung are shown. **B,** percentage of mice with metastasis is indicated in the graph ($n = 8$ per group). **C,** quantification of circulating GFP^+ tumor cells (CTC). **D,** quantification of circulating $DsRed^+$ fibroblast cells (CFC). In **B** and **C,** *, $P < 0.05$ vs. tumor alone; in **D**, *, $P < 0.05$ vs. tumor + CAF. **E,** sections of metastatic nodules from tumor plus CA-MSC liver stained with anti-GFP. **F,** sections of metastatic nodules from tumor plus CA-MSC liver stained with anti-RFP antibody. Inset showing RFP-labeled MSC next to GFP-labeled proliferating tumor cells, and both RFP-and GFP-labeled cells next to blood vessels (BV).

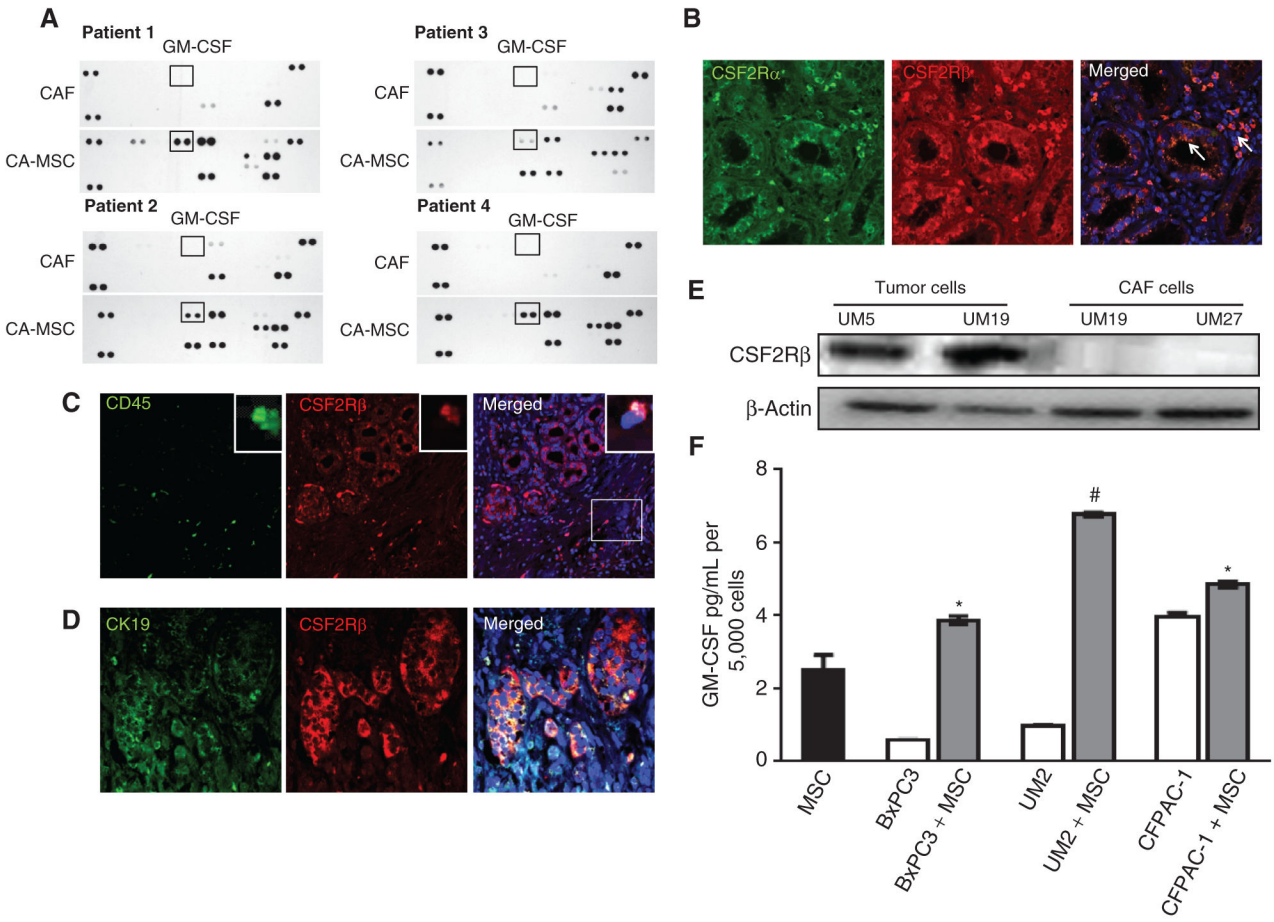

Figure 4.

CA-MSCs differentially secrete GM-CSF. Human cytokine arrays showing the cytokine expression of human primary pancreatic CAFs and CA-MSCs (MSC) from 4 patients with pancreatic cancer. **A,** differential expression of GM-CSF by CA-MSCs was present in all 4 patient samples. **B,** immunofluorescent staining for the GM-CSF receptors CSF2Rα (green) and CSF2Rβ (red) in human PDA tissue sections. Nuclei are stained with DAPI (blue). **C,** immunofluorescent staining for CD45 (green) used to identify immune cells and CSF2Rβ (red) in human PDA tissue sections. **D,** immunofluorescence staining for CK19 (green) to identify ductal cells and CSF2Rβ (red) in human PDA tissue sections. **E,** Western blots showing differential expression of GM-CSF receptors in tumor and CAF cells. **F,** ELISA data quantifying amount of GM-CSF secreted by KRAS wild-type (BxPC-3) and KRAS-mutant (UM2 and CFPAC-1) tumor cells and CA-MSCs (data expressed as mean ± SEM; *, $P < 0.0001$ compared with BxPC-3 alone; #, $P < 0.0001$ compared with UM2 alone; and +, $P < 0.005$ compared with CFPAC-1 alone).

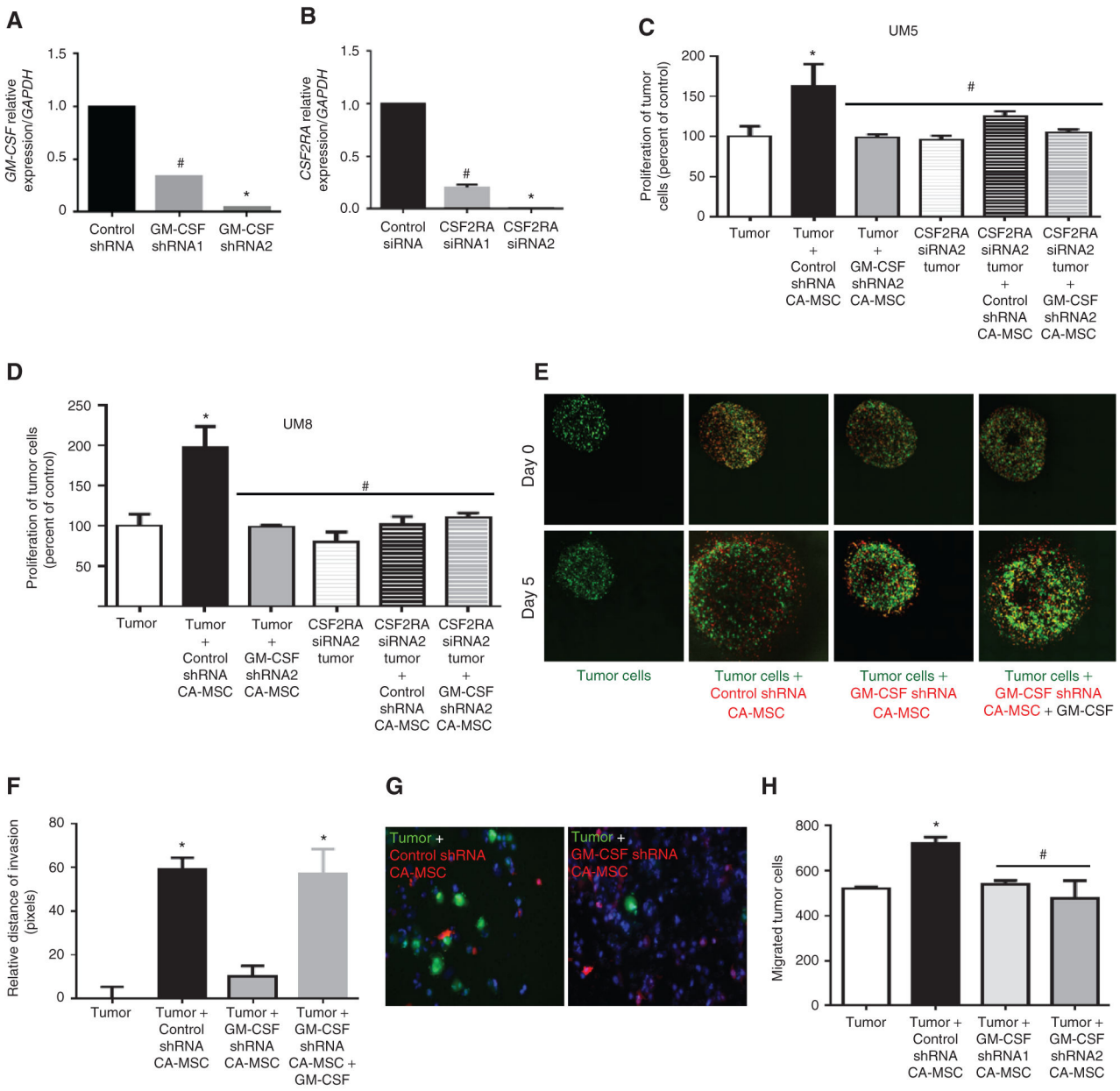

Figure 5.

GM-CSF from CA-MSCs is required for tumor cell invasion and transendothelial migration. **A,** levels of *GM-CSF* mRNA in CA-MSCs expressing control shRNA or GM-CSF shRNA 1 or 2. **B,** levels of *CSFR2A* mRNA in tumor cells expressing control siRNA or CSF2RA siRNA 1 or 2. **C,** increased proliferation of UM5 tumor cells when cultured with CA-MSC cells expressing control vs. GM-CSF shRNA (data expressed as mean ± SEM; $n = 3$; *, $P < 0.0002$ compared with UM5 control; #, $P < 0.0002$ compared with UM5 tumor cell + GM-CSF shRNA CA-MSC). **D,** increased proliferation of UM8 tumor cells when cultured with CA-MSC cells expressing control vs. GM-CSF shRNA (*, $P < 0.001$ compared with UM8 control; #, $P < 0.001$ compared with UM8 tumor cell + GM-CSF shRNA CA-MSC). **E,** collagen invasion assays in GFP-labeled tumor cells alone, tumor cells + control shRNA

CA-MSC, tumor cells + GM-CSF shRNA CA-MSCs, and exogenous GM-CSF added to tumor cells + GM-CSF shRNA MSCs. CA-MSCs are labeled with DsRed. **F,** the invasion of tumor cells was significantly increased in the presence of CA-MSC cells. This increase in invasion index was inhibited with GM-CSF knockdown in MSCs and rescued with exogenous GM-CSF (data expressed as mean ± SEM; $n = 3$; *, $P < 0.0001$ compared with control). **G,** microscopic images showing enhanced migration through an endothelial layer of tumor cells + control shRNA CA-MSC compared with tumor cells + GM-CSF shRNA CA-MSCs [GFP-labeled tumor cells (green), DsRed-labeled CA-MSC cells (red), and nuclei stained with DAPI (blue)]. **H,** quantification of tumor cells migrating through the endothelial layer under different treatment conditions. Increase in tumor cell migration when cultured with CA-MSCs expressing control vs. GM-CSF shRNA (data expressed as mean ± SEM; $n = 3$; *, $P < 0.001$ compared with control; #, $P < 0.01$ compared with tumor + GM-CSF shRNA CA-MSC).

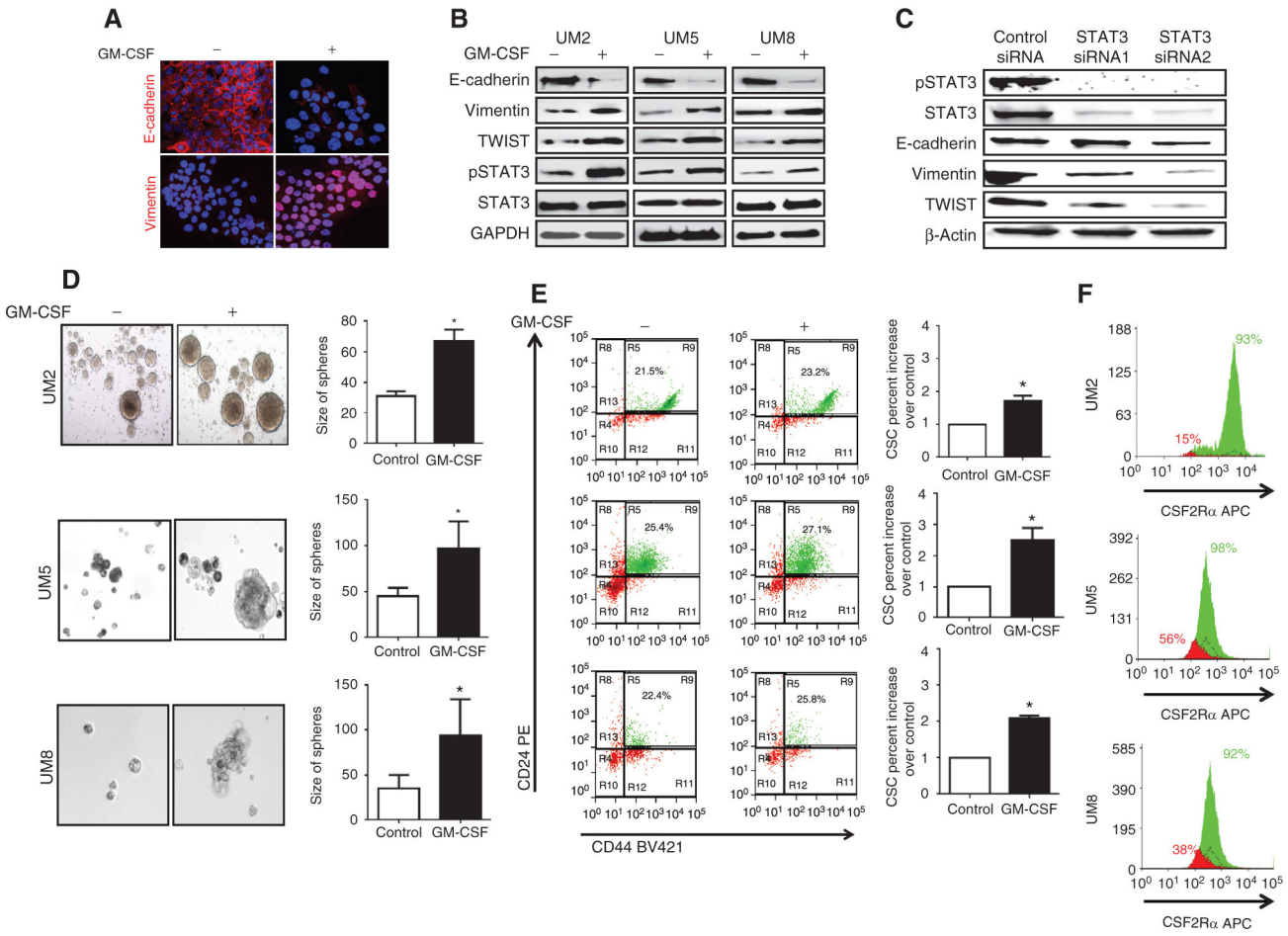

Figure 6.

GM-CSF induces tumor cell EMT and stemness. **A,** IHC staining of UM5 tumor cells for the epithelial marker E-cadherin and mesenchymal marker vimentin following treatment with exogenous GM-CSF (100 ng/mL). **B,** Western blotting for EMT markers and phosphorylated (p) and total STAT3 in the UM5, UM2, and UM8 pancreatic cancer cells treated with exogenous GM-CSF. **C,** Western blot evaluating expression of EMT markers in either control or STAT3 siRNA (1 and 2) UM5 cells treated with GM-CSF. **D,** enhanced size of tumorspheres when UM5, UM2, and UM8 tumor cells were treated with 100 ng/mL GM-CSF (*, $P < 0.0001$ vs. control for UM5; *, $P < 0.0001$ vs. control for UM2; *, $P < 0.004$ vs. control for UM8). **E,** FACS analysis revealed an increase in the percentage of CSCs (ESA^+ $CD44^+$ $CD24^{+)}$ when cultured in the presence of exogenous GM-CSF (100 ng/mL; *, $P < 0.05$ vs. control for UM5; *, $P < 0.02$ vs. control for UM2; *, $P < 0.0001$ vs. control for UM8). **F,** FACS analysis for CSF2Rα receptor expression in CSCs (green) and bulk cells (red) showing significantly higher number of CSCs (green) expressing GM-CSF receptor than the bulk tumor cell population (red).

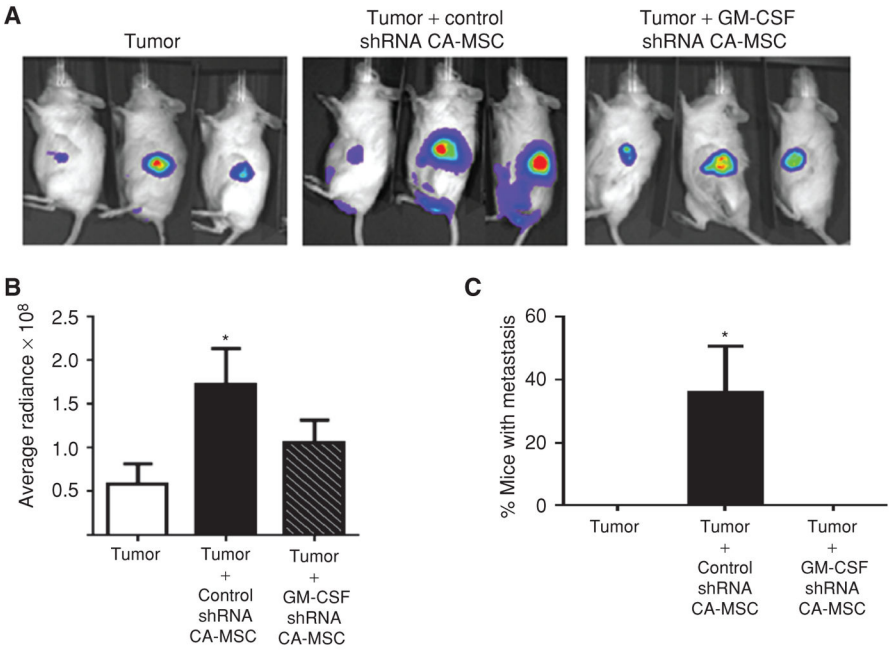

Figure 7.

GM-CSF is required for CA-MSC–induced tumor metastasis. Pancreatic cancer cells transduced with a luciferase-expressing lentivirus were orthotopically injected alone or with CA-MSCs expressing control or GM-CSF shRNA-2 into the pancreatic tail of NOD/SCID mice ($n = 5$ per group). **A,** representative bioluminescent images of animals in each group are shown 3 weeks after injection depicting tumor burden. **B,** bioluminescent-based tumor growth from tumor cells alone or in combination with CA-MSCs expressing control or GM-CSF shRNA. Pooled results of the average tumor size ± SEM from each group. **C,** percentage of mice with metastasis in each group is indicated ($n = 5$ per group; *, $P < 0.05$ vs. tumor alone).